



## Physical properties of craters on asteroid (21) Lutetia

Jean-Baptiste Vincent<sup>a,\*</sup>, Sébastien Besse<sup>b</sup>, Simone Marchi<sup>c</sup>, Holger Sierks<sup>a</sup>, Matteo Massironi<sup>d</sup>,  
The OSIRIS Team<sup>1</sup>

<sup>a</sup> Max-Planck-Institut für Sonnensystemforschung, Max-Planck-Strasse 2, 37191 Katlenburg-Lindau, Germany

<sup>b</sup> Department of Astronomy, University of Maryland, MD 20742-2421, USA

<sup>c</sup> Université de Nice – Sophia Antipolis, Observatoire de la Côte d'Azur, CNRS, 06304 Nice, France

<sup>d</sup> Università di Padova, Dipartimento di Geoscienze, Padova, Italy

### ARTICLE INFO

#### Article history:

Received 25 June 2011

Received in revised form

9 December 2011

Accepted 28 December 2011

#### Keywords:

Lutetia

Asteroid

Craters morphology

Regolith

### ABSTRACT

This paper presents an analysis of the physical properties of craters on asteroid (21) Lutetia, derived from images acquired by OSIRIS, the high-resolution cameras onboard ESA's spacecraft Rosetta. Crater morphology on (21) Lutetia fits very well with the general picture of what was known for previously visited small bodies, with a typical depth to diameter ratio of 0.12. We discuss here the distribution of this parameter all across the surface, but also region by region, and see how it can vary from one location to another and help to distinguish between different geological units. In a later section of the paper we study in more details Beatica region where a deep ejecta blanket filled most of the craters, and estimate the thickness profile of this ejecta based on our analysis of the  $d/D$ . We find a good agreement with existing scaling laws, and use this to constrain the scale of the original event that reshaped the surface around the North pole of the asteroid. Finally, we report on the observations of avalanches in several crater flanks, and the presence of many asymmetrical craters with flow-like features, and discuss the evidence for widespread fine material all over the surface.

© 2012 Elsevier Ltd. All rights reserved.

### 1. Introduction

Since the discovery of (1) Ceres by Giuseppe Piazzi in 1801, more than one million minor planets have been detected in our Solar System, but it is only in the last 20 years that their surface could be resolved in detail with in situ observations. Starting with the visit of (951) Gaspra by Galileo in 1991, 10 asteroids have been imaged by a spacecraft (Table 1), the latest encounter being rendez-vous of DAWN with (4) Vesta in July 2011. As any other atmosphereless bodies, asteroid surfaces display a record of impact events that occurred since the early days of their formation. From the Apollo epoch, craters and their statistical distribution across the surface of a planet are studied in order to date the surface, derive its chronology, and constrain the dynamical evolution of the asteroid belt, or more generally the Solar System. Although this topic is of great interest, the age determination has already been presented in a companion paper by Marchi et al.

(this issue) and we focus here on crater morphology rather than count or distribution. Since a crater is formed when an impactor collides with the surface, its physical properties are determined first by the impactor properties (size and velocity) and the local structure of the surface (material, strength, and porosity). In addition, the original morphology of the crater will be affected by aging processes. For instance existing craters can be erased or modified by subsequent impacts or vibrations (Richardson et al., 2005). Some asteroids like (243) Ida (Chapman et al., 1996) display many craters whereas others like (25143) Itokawa are almost devoid of impact features (Hirata et al., 2009). It is worth noting that (433) Eros (Thomas et al., 2002) shows many impact craters but presents a lack of small ones, which could have been erased by processes mentioned above. Similar processes may have occurred on (2867) Steins as well (Marchi et al., 2010). Therefore the understanding of cratering on asteroids is not straightforward. Study of crater morphology can be seen as an tool to derive not only ages, but also physical properties of a surface, and add constraints on the underlying structure of the asteroid and its evolution.

In the following sections, we will present first the data and discuss the technique we used to study the crater morphology of (21) Lutetia. We will move then to a statistical descriptions of the measurements and establish a comparison with existing work on other small bodies of the Solar System. Finally we will discuss the

\* Corresponding author. Tel.: +49 5556 979 539.

E-mail address: [vincent@mps.mpg.de](mailto:vincent@mps.mpg.de) (J.-B. Vincent).

<sup>1</sup> M. A'Hearn, F. Angrilli, C. Barbieri, A. Barucci, J.-L. Bertaux, G. Cremonese, V. Da Deppo, B. Davidsson, S. Debei, M. De Cecco, S. Fornasier, M. Fulle, O. Groussin, P. Gutierrez, S.F. Hviid, W.-H. Ip, L. Jorda, H.U. Keller, D. Koschny, J. Knollenberg, J.R. Kramm, E. Kuehrt, P. Lamy, L.M. Lara, M. Lazzarin, J.J. Lopez-Moreno, F. Marzari, H. Michalik, G. Naletto, H. Rickman, R. Rodrigo, L. Sabau, N. Thomas, K.-P. Wenzel.

**Table 1**  
List of asteroids visited by spacecrafts.

| Object            | Year of visit | Mission      |
|-------------------|---------------|--------------|
| (951) Gaspra      | 1991          | Galileo      |
| (243) Ida, Dactyl | 1993          | Galileo      |
| (253) Mathilde    | 1997          | NEAR         |
| (9969) Braille    | 1999          | Deep Space I |
| (433) Eros        | 2000          | Near         |
| (5535) Annefrank  | 2002          | Stardust     |
| (25143) Itokawa   | 2005          | Hayabusa     |
| (2867) Steins     | 2008          | Rosetta      |
| (21) Lutetia      | 2010          | Rosetta      |
| (4) Vesta         | 2011          | DAWN         |

**Table 2**  
Description of the images used to identify craters and measure their morphological parameters. Time is given with respect to the closest approach.

| Image name                        | Scale<br>(m/px) | Phase angle<br>(°) | Time<br>w.r.t. CA (s) |
|-----------------------------------|-----------------|--------------------|-----------------------|
| NAC-2010-07-10T15.42.47.523...F22 | 65              | 51                 | −114                  |
| NAC-2010-07-10T15.43.35.802...F22 | 60              | 63                 | −66                   |
| NAC-2010-07-10T15.45.09.210...F22 | 58              | 87                 | +88                   |

implication of this study for the history of (21) Lutetia and the physical properties of its surface.

## 2. Data and technique

The study is based on data acquired by the OSIRIS cameras onboard Rosetta (Keller et al., 2007). On its way to comet 67P/Churyumov–Gerasimenko, the spacecraft flew by two asteroids: (2867) Steins on 5 September 2008 (Keller et al., 2010) and (21) Lutetia on 10 July 2010, the latter being the second largest asteroid ever visited by a spacecraft (Sierks et al., *accepted for publication*). During the fly-by, the OSIRIS imaging system took more than 400 pictures through its wide (WAC) and narrow (NAC) angle cameras, covering slightly more than 50% of the asteroid surface, mostly the Northern hemisphere. At the closest approach (3170 km), the resolution of NAC images was as good as 60 m/px, revealing the very complex morphology of the asteroid and its craters in great detail.

For the following analysis we used three NAC images only, acquired shortly before and after the closest approach (see Table 2 for details). This set gave us the highest resolution images of craters in the observed hemisphere. The phase angle varying from 51° to 87° allowed us to measure precisely the crater parameters in different viewing conditions, for better accuracy.

Due to the high spatial resolution, most of the craters could be identified directly on raw images, but we cross checked the selection using enhanced/filtered versions of the same images. Sharpening by unsharp masking, and/or filtering with a Laplacian was used to detect all craters, even the partially buried ones, which had the lowest contrast. Among all the parameters one can measure, we wanted to retrieve mainly the depth-to-diameter ratio ( $d/D$ ).

The physics leading to the formation of the crater is different depending whether the cratering regime is strength or gravity dominated. For the transient cavity, the transition diameter between the two regimes can be estimated through scaling laws like one derived by Asphaug et al. (1996):  $D_{trans} \sim 0.8Y/g\rho$ . From the shape model provided by Jorda et al. (2010) we calculated the gravitational acceleration at the surface of Lutetia, assuming an homogeneous density of  $\rho = 3400 \text{ kg m}^{-3}$  (see Sierks et al.,

*accepted for publication*), and derived a maximum value of  $g = 0.049 \text{ m s}^{-2}$ . Assuming a typical rock strength of  $Y = 2 \times 10^7 \text{ N m}^{-2}$  (Rummel et al., 1987) we obtain a transition diameter of 96 km, which is about the diameter of Lutetia. Therefore on this asteroid where the largest observed crater has a diameter of 55 km, all craters fall into the strength-dominated regime and we expect the variation of depth with respect to diameter to follow the near linear power law  $d = aD^b$ , with  $b \cong 1$  (Grieve, 2007) and  $a$  a constant for a given terrain. This ratio depends on properties of both impactor (structure and velocity) and local surface (strength and structure). In principle  $d/D$  reflects mainly the variation of surface properties, and can help us to better identify or constrain different geological units. Note that  $d/D$  somewhat reflects also the age of the surface, as old craters tend to be eroded, larger and less deep than fresh ones. This must be taken in consideration when interpreting the statistical study.

We identified more than 350 craters across the surface but this paper uses only 125 of them, distributed all over the regions of interest (Fig. 1). These craters were selected for being the only ones where we could measure accurately both depth and diameter at the same time. Diameters were measured by manually selecting at least 5 points on the rim of each crater and fitting an ellipse to these points; the largest axis of the ellipse being considered as the true crater diameter (Fig. 2, panel A). Depth was estimated from the shadows with the following relation:  $d = L \times \tan(\theta_s)$ ,  $L$  being the projected length of the shadow and  $\theta_s$  the local solar elevation in the region surrounding the crater. We used for this a low resolution shape model of (21) Lutetia created by Jorda et al. (2010). Using the latest SPICE kernels describing the orbit of the spacecraft during the fly-by, we oriented properly the shape model and projected our images on it (Fig. 2, panel B). This allowed us to know precisely all the necessary angles, in particular the local solar elevation at each point of the surface. From there one can easily convert the length of shadows to vertical height with the trigonometric relation cited above.

It is important at this point to discuss the errors inherent to such measurement. Craters rim are usually sharp and easily identified in the images; repeated measurements of diameter

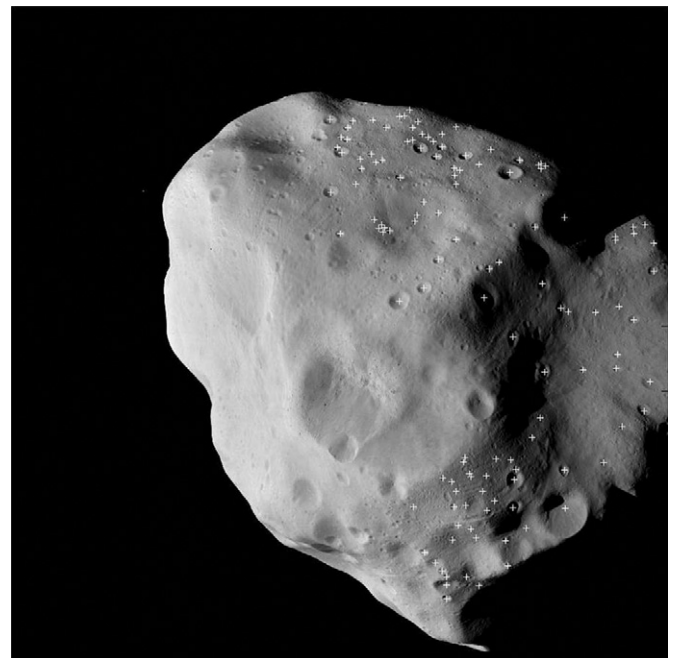


**Fig. 1.** Display of all craters included in our study. They are marked by white crosses on this image of Lutetia taken 1 min before the closest approach.

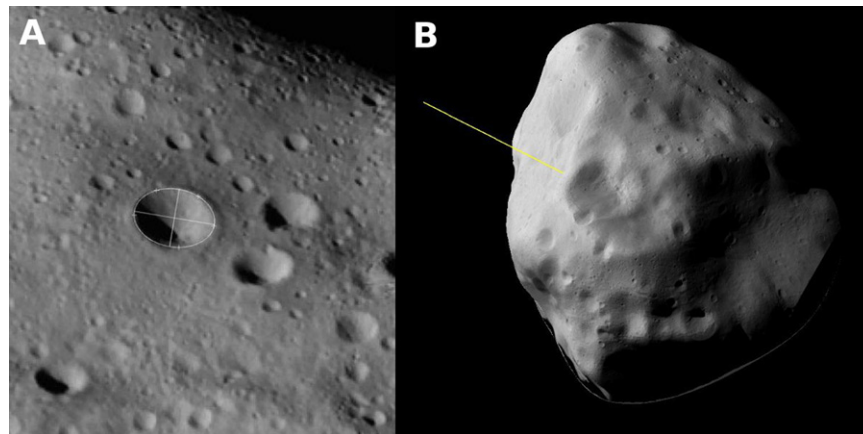


**Fig. 2.** Method used to measure crater parameters. Panel A shows an ellipse fitted to one of the studied craters. Panel B displays a projection of one image of Lutetia on top of the shape model. The yellow line indicates the direction of the Sun at the time when this specific image was taken. This gives us directly the precise value of the solar elevation with respect to a given area of the surface at any time.

for a same crater do not differ by more than two pixels (i.e. about 120 m). Depth is more difficult to retrieve and suffer from two sources of error. One is the measurement of the shadows, and is the same as for the estimation of the diameter. It is more difficult to quantify the error from the shape model itself but it is generally assumed to be less than 20% for local slopes (Carr et al., 1994). However we measure here the solar elevation with respect to slopes averaged over large regions of the asteroid and this error becomes negligible. At large scales different shape reconstruction techniques produce the same slopes with less than 5% difference (Jorda, personal communication). The final error on the depth is at maximum 10%, and propagates into a maximum uncertainty of 0.037 on the  $d/D$  ratio for the craters studied. All values of  $d/D$  described later will assume this same uncertainty. As a test we also compared our measurements with an independent estimation of  $d/D$  based on a digital terrain model by Preusker et al. (this issue) obtained by stereographic reconstruction and found a perfect agreement between the results.

### 3. Physical properties of craters

Fig. 3 shows one of the images used, with solid lines indicating the main geological units identified on the surface of Lutetia (Sierks et al., accepted for publication). Our study focuses on four main regions, namely Achaia, Noricum, Narbonensis, and Baetica. Achaia is believed to be the oldest region in the Northern hemisphere, it has the highest crater density and presents a flat and relatively undisturbed topography. Noricum is somehow similar in terms of crater density but displays a very complex morphology and is the region of Lutetia where one can identify many diverse geological features such as grooves and grabens (Thomas et al., this issue). Narbonensis contains Massilia; the largest (55 km diameter) crater seen on Lutetia, and small craters present in this regions show different features than those in other regions. Finally Baetica is depleted of craters, apart from a large (21 km diameter) crater cluster which covered all the region in a deep ejecta blanket.

Fig. 4 presents an histogram summarizing our measurements of  $d/D$ . We observed values ranging between 0.05 and 0.3 and following a Gaussian distribution peaking at 0.12. When this ratio is plotted with respect to the crater diameter (Fig. 5), we note that craters larger than 4 km are usually close to the mean value of 0.12, whereas small craters cover all the range of  $d/D$ . This

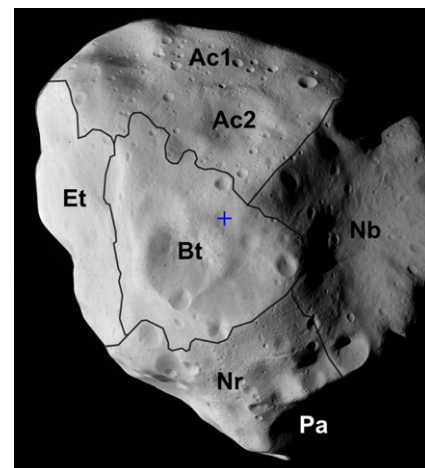


**Fig. 3.** Image acquired 1 min before the closest approach showing six of the eight different regions of (21) Lutetia, as presented in Sierks et al. (accepted for publication) and validated by the IAU. Ac, Achaia (divided into two subunits Ac1 and Ac2); Bt, Baetica; Et, Etruria; Nb, Narbonensis; Nr, Noricum; Pa, Pannonia. The blue cross indicates the North pole position. (For interpretation of the references to color in this figure legend, the reader is referred to the web version of this article.)

threshold is however only a qualitative value since there are not enough large craters to constrain it properly.

Broken down to individual regions, the plots of depth with respect to diameter show interesting features (Fig. 6).

- Achaia displays clearly two independent linear trends of  $d/D$  (Fig. 6, top panel), with average values of 0.117 and 0.176. When looking for the spatial distribution of craters belonging to these two trends, we find them to be clearly separated in two subunits (Ac1 and Ac2 in Fig. 3). Shallow craters are found in the subregion showing a larger density of craters, deeper craters are located in another subregion marked by the presence of two very large and shallow depressions about 10 and 20 km that could be old craters.
- Noricum shows a complex distribution of  $d/D$  (Fig. 6, bottom panel). As a very first approximation the values follow a linear trend with a mean  $d/D = 0.166$ , but many craters are much deeper than expected from the average linear trend. On a topographic level, this region is very different from Achaia and

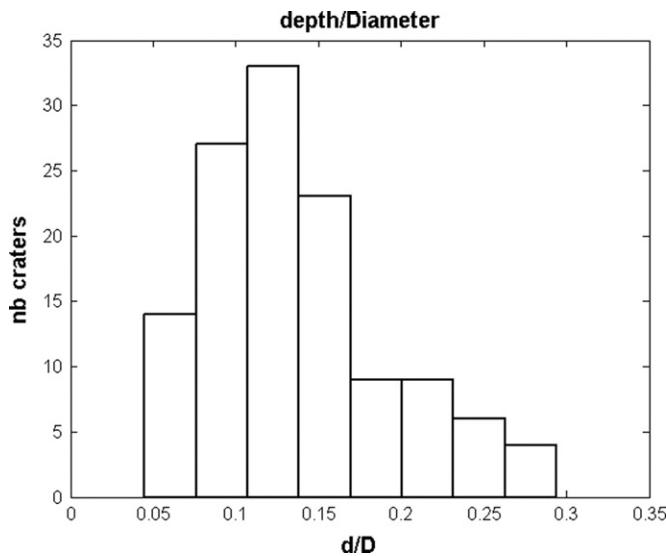


**Fig. 4.** Histogram of depth-to-diameter values for the whole surface. The distribution peaks at 0.12. The extreme cutoffs at 0.05 and 0.3 are independent of the binning used to display the histogram.

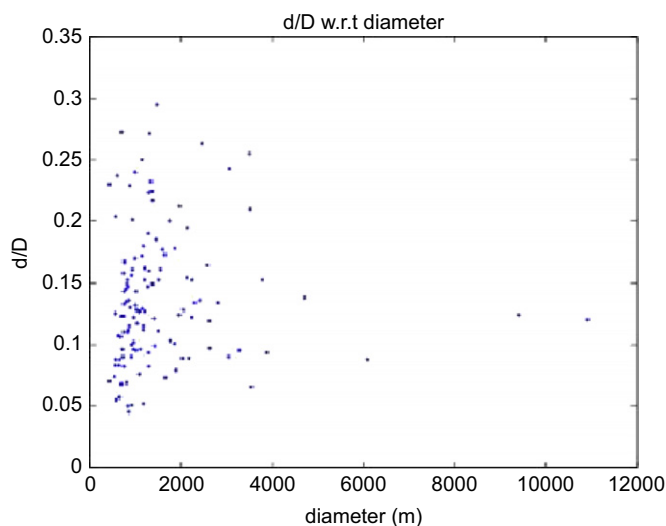


**Fig. 5.** Plot of  $d/D$  with respect to diameter. Large craters have a  $d/D$  close to the 0.12 peak of the distribution whereas small craters cover all the range of  $d/D$ .

displays a very complex morphology, in particular deep grooves and grabens.

- Narbonensis presents a linear variation of depth with respect to diameter (Fig. 7). Craters are shallow with a typical  $d/D$  of 0.118, i.e. similar to the main subunit of Achaia.
- Baetica does show too few and small craters to measure properly the  $d/D$ . These craters appear to be extremely fresh and are usually only a few pixels in diameter, i.e. a few hundred meters at most. Other features of this region will be discussed at length in the next section.

The quality of the fits can be estimated in different ways. We use here the reduced  $\chi^2$ , defined as  $\chi^2/(N-n-1)$  where  $N$  is the number of observations and  $n$  the number of variables in the fit. The fit is good if this value is close to one. For Ac1, Ac2, Nr, and Nb, we found a respective  $\chi^2_{red}$  of 1.002, 1.161, 1.077, and 1.087.

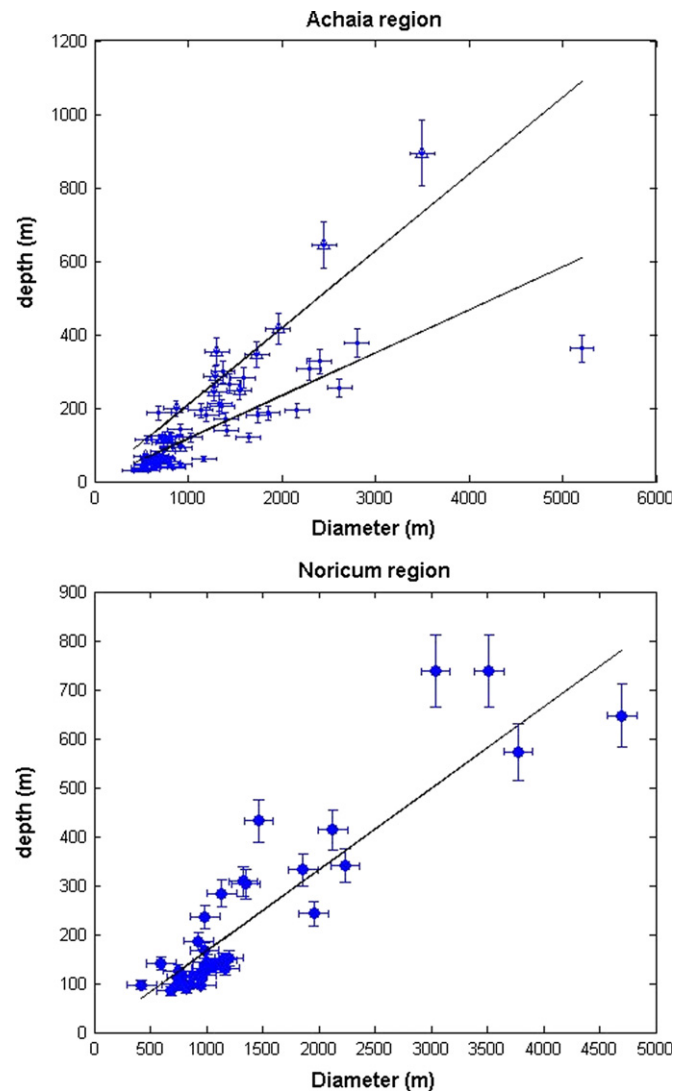


**Fig. 6.** Plots of depth w.r.t. diameter for the regions studied. The solid lines indicate the general trend of the data, based on the average  $d/D$  ratio of each region. Notice that two trends can be identified in Achaia, and that Noricum is far from the expected linear behavior.

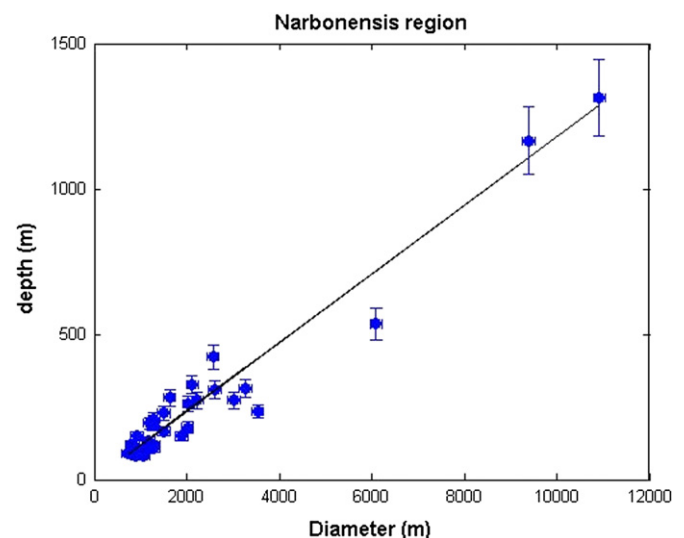


**Fig. 7.** Fig. 6 continued. The distribution of  $d/D$  for Narbonensis displays a remarkable linear trend.



#### 4. Implication for the physical properties of the surface and Lutetia history

##### 4.1. General considerations

As for crater morphology, Lutetia fits perfectly with what we know of other surfaces of airless bodies in the Solar System. Values and distribution of  $d/D$  fall in the expected range (see Table 3 for a comparison with fresh craters in other Solar System objects). The variations of  $d/D$  across Lutetia can be interpreted not only as differences in the physical properties of the surface, but also as differences in the evolutionary processes that affected different locations of the asteroid. Indeed craters tend to become shallower with time, due to erosion, or flattening by seismic shaking or subsequent impacts. These effects deteriorate the rims of the craters and fill the interior with material, leading to an increase in diameter and a decrease in depth, i.e. a smaller  $d/D$ . However here we find differences for regions with a similar crater density, i.e. age. Therefore we believe that differences in  $d/D$  are mainly due to local changes in surface properties. It is striking for instance to observe how  $d/D$  departs from a linear fit in the Noricum region where the geomorphology indicates that strong events reshaped the surface, possibly creating deep fractures. On the opposite side, regions appearing to have had a more quiet morphological evolution (Achaia and the floor of Massilia crater) show a remarkable linear trend. Differences observed in subunits of Achaia are very well correlated to the presence of two possible large craters. Therefore this makes us confident in using  $d/D$  as a diagnostic tool to better identify or constrain geological units at the surface of the asteroid.

##### 4.2. Thickness of ejecta blanket in Baetica

In the special case of Lutetia, these measurements lead to a further analysis of the surface physical properties. As discussed before, Baetica region is covered with a thick layer of ejecta blanket, which filled most of the pre-existing craters. However the outline of some of these buried craters can be clearly identified in our images and we can measure their diameter. Since these craters were present before the event that resurfaced Baetica, and have then been filled by ejecta, if we can estimate their original depth we can in principle derive the thickness of material that fell into the crater. This of course assumes that we know what was the original  $d/D$  ratio in this region. We do not have any way to know this value for sure and it could be in theory anywhere between 0.05 and 0.3 (the range of values observed everywhere else on Lutetia). However one can constrain this parameter with the following arguments: looking at the distribution of linear features on the surface, it appears that very few, if any, would have crossed the region before its resurfacing. Therefore we expect the former surface to have relatively undisturbed, and closer to the physical properties of Achaia than Noricum. Measurement of  $d/D$  values at the border of the region, where the ejecta ends, is all in the peak of the distribution of  $d/D$  as shown in Fig. 4. Hence we used the most probable value of  $d/D = 0.12$  to

estimate the original depth of the buried craters, as it was before the event that filled them with ejecta. Applied to the largest one, this leads to a maximum ejecta thickness of  $\sim 600$  m. Note that we took into account the fact that some of these craters are not completely filled and we removed the non-filled part from our estimations. Using this principle we propose a possible profile of the depth of ejecta for the whole region (see Fig. 8). We obtain the two following conclusions:

(1) Our measurements of the thickness profile for the ejecta blanket are fitted best with the following power law:

$$B(r) = 560 \left( \frac{r}{R_{crater}} \right)^{-2.68} \quad (\text{m}) \quad (1)$$

where  $B(r)$  is the thickness of ejecta at a distance  $r$  from the crater center.

Craters properties can be quantified analytically with the theory developed by Housen et al. (1983). In a strength dominated regime, the solution describing the thickness of the ejecta blanket with respect to the distance from the crater center is a decreasing power law of the type:

$$\frac{B(r)}{R_{crater}} = K \left( \frac{Y}{\rho g R_{crater}} \right)^{e_v/2} \left( \frac{r}{R_{crater}} \right)^{-e_r} \quad (2)$$

$$K = K_4 \frac{(e_r - 2)}{2\pi} \sin(2\theta)^{e_r - 2} \quad (3)$$

Exponents  $e_r$  and  $e_v$  are defined as  $e_v = 2e_r - 4$  and  $e_r$  is a constant for a given combination of target and projectile material, typically between 2.5 and 3.  $K_4$  is an other constant used to quantify the volume,  $V_e$ , of ejecta launched with a velocity greater than an arbitrary value  $v$ .

$$\frac{V_e}{R^3} = K_4 \left( v \sqrt{\frac{\rho}{Y}} \right)^{-e_v} \quad (4)$$

Housen et al. (1983) and Housen and Holsapple (2011) performed an extensive analytical and experimental study of cratering laws. They report a value of  $0.05 < K_4 < 0.08$  for strength dominated impacts.  $Y$ ,  $\rho$ , and  $g$  are the same as defined in Section 2.

It is important to note that the whole description of ejecta thickness with respect to distance from the crater center is

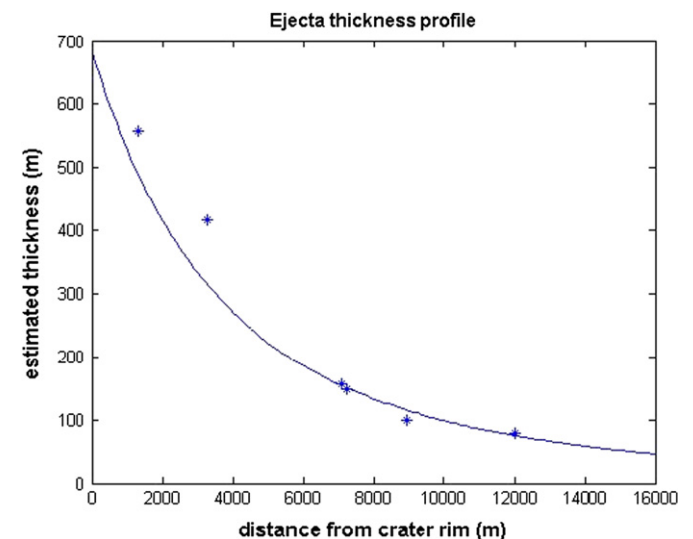


**Fig. 8.** Estimated thickness profile of the ejecta blanket in Baetica region. Stars represent the estimated depth of several buried craters in the region, based on the assumption that their initial  $d/D$  was equal to 0.12 (typical value for Lutetia). The solid line shows the best fit of a power law, seemly Housen et al. (1983) scaled to Lutetia.

**Table 3**  
Depth-to-diameter ratio of simple craters for other Solar System objects.

| Object             | $d/D$     | Reference                                |
|--------------------|-----------|--|
| (951) Gaspra       | 0.12      | Carr et al. (1994)                       |
| (243) Ida          | 0.153     | Sullivan et al. (1996)                   |
| (253) Mathilde     | 0.12–0.25 | Veverka et al. (1999)                    |
| (433) Eros         | 0.14      | Veverka et al. (2000)                    |
| Moon, Mars, Phobos | 0.2       | Shingareva et al. (2008)                 |
| (2867) Steins      | 0.04–0.25 | Besse et al. (submitted for publication) |

reduced to a function of physical parameters of the surface, and two constants  $e_r$  and  $K_4$ .

Our fit of the data is in good agreement for the exponent  $e_r$ , which is found in the expected range.

By equalizing Eqs. (1) and (2) we can calculate the other constants. Doing so we find exactly  $K_4 = 0.08$ , again in perfect agreement with the work by Housen et al., hence their analytical theory can be applied directly to Lutetia.

Integrating the thickness of ejecta all around the crater, we estimate a total volume of  $3 \times 10^{11} \text{ m}^3$ . With a typical  $d/D$  of 0.12,

this amount of material would fit in a crater of 21.2 km diameter which is exactly the scale of the latest impact in Baetica (21 km).

(2) The same formula (Eq. (1)) can be used to estimate the extent of the spatial distribution of continuous ejecta. The end of the ejecta blanket is materialized by a transition between smooth and rough terrain. With a resolution of 65 m/px and the Sun elevation being about  $50^\circ$  in this area of Lutetia when images were acquired, the smallest feature we can detect (i.e. that can create at least 1 pixel of shadow) would have an elevation of 55 m. According to the scaling law, this would happen at 26 km from the crater center, which is consistent with our observations (Fig. 9).

#### 4.3. Avalanches and other dry granular flows

Finally, another important physical property of the surface that can be derived from the study of craters is the grain size. Several craters on Lutetia display granular flows in their inner flanks (Fig. 10), on slopes less or equal to  $33^\circ$  with respect to the local gravity field. As this value is approximatively the maximum angle of repose of sand, this implies that the material seen flowing down in the avalanches must be made of fine grains. This idea is supported by the presence of peculiar craters found in Narbonensis (Fig. 10). They are not only shallower than in other regions but also display an typical asymmetric shape, one half of the crater rim being very sharp, and the opposite edge very soft with a flow-like shape. Such craters can be explained with several possible mechanism:

- A shallow impact ( $< 15^\circ$ ) would produce an elliptic crater but it cannot explain the asymmetry found only in this region. There are elliptical craters in other places in the Northern hemisphere of Lutetia but they show a very consistent rim all around and do not display this flow-like structure. A large fraction of oblique impacts is also unlikely.
- Structural control made by pre-existing planes of weakness. It is important in Lutetia since it controls also the asymmetric shape of at least two big craters of the polar region (Massironi et al., this issue) however for the Narbonensis craters, this can be ruled out as there are no linear features which could be associated with the observed irregularities.
- Impact into fluffy material would also lead to a splash of regolith flowing along the local gravity vector and the outer

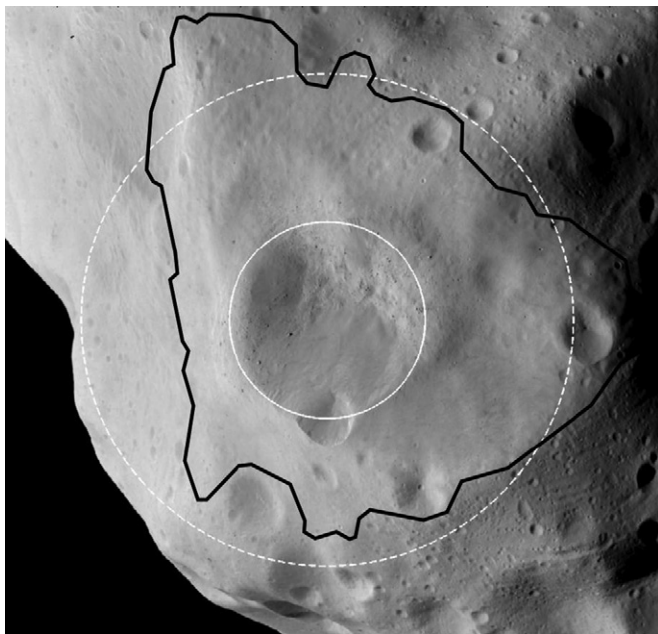


**Fig. 9.** Close view of the North pole crater cluster in Baetica region. Field of view is  $45 \times 45 \text{ km}$ . Notice that this region is almost devoid of small craters. A few impacts are visible but almost completely buried under a thick ejecta blanket. The white solid line represents the central 21-km-diameter crater. The dashed line is the projected limits for the continuous ejecta deposit, according to the scaling law defined in Section 4.2. The black solid line marks the limit of the actual ejecta blanket, defined as the region surrounding the crater where ejecta covered and smoothened out topographic features with respect to the rougher terrain further away from the crater.

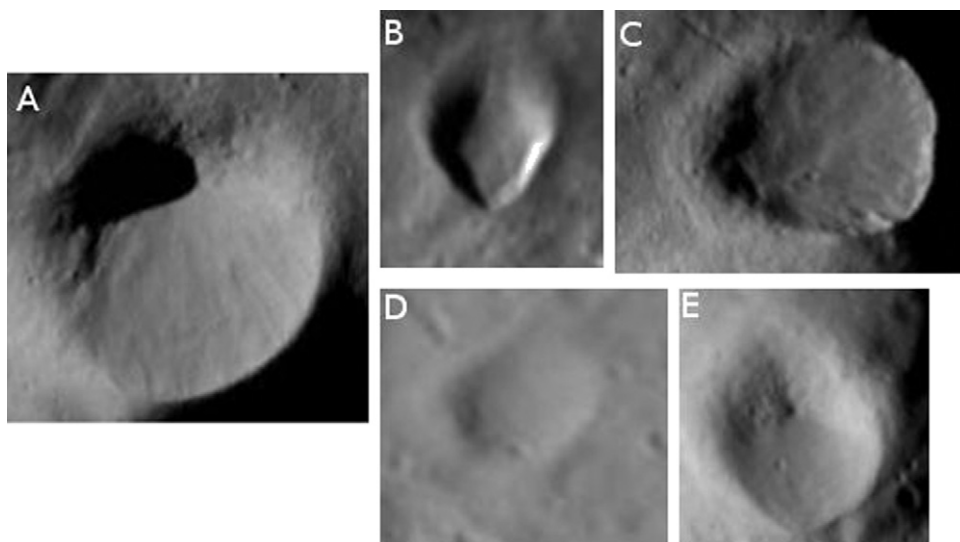


**Fig. 10.** Dry granular flows on Lutetia. Panel A shows avalanches on the flanks of a 10 km diameter craters. Panels B–E present smaller crater (about 5 km diameter) seen in Narbonensis region, which is a very peculiar asymmetric shape where one edge of the rim seems to flow away from the crater.

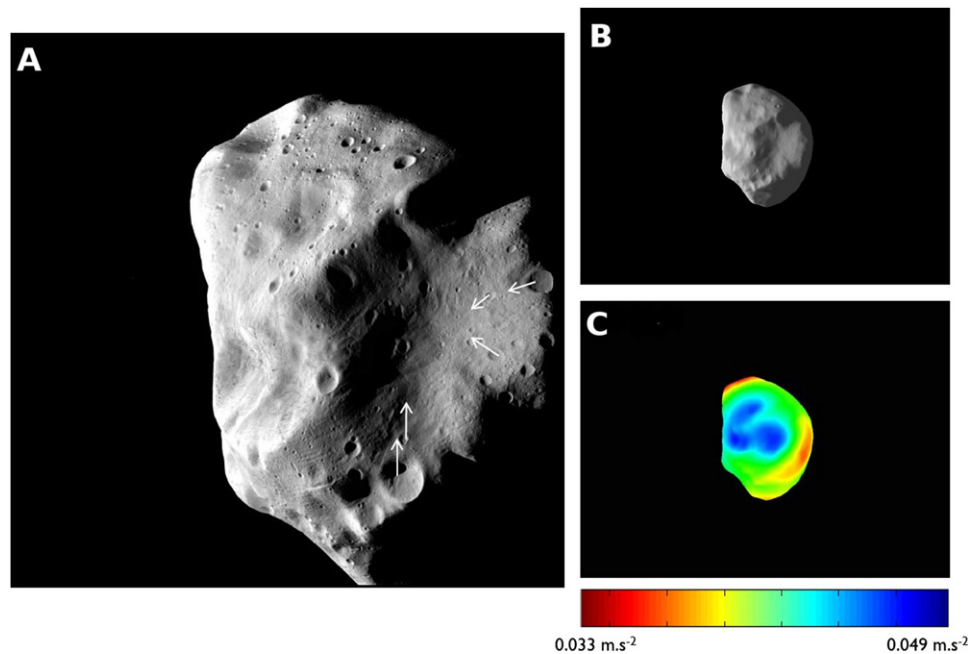


**Fig. 11.** Panel A shows Location and orientation of the asymmetric craters inside Narbonensis. The flows are all pointing towards the center of the large crater, and follow the local gravity field. Panels B and C display respectively the shape model by Jorda et al. (2010) and the gravity field of Lutetia. Colors indicate the strength of the gravity field vector in the fixed frame of Lutetia. As the gravity vector is negative in this frame, strong values are indicated in blue and weaker ones in red. Material is flowing towards the lowest gravitational potential, i.e. regions coded in blue in the figure. (For interpretation of the references to color in this figure legend, the reader is referred to the web version of this article.)

crater flanks. To test this hypothesis we plotted the direction of the flows in Fig. 11 and calculated the local gravity field based on the low-resolution shape model by Jorda et al. (2010). We found a very good correlation, supporting the idea that we see granular flows in Narbonensis.

## 5. Conclusion

To summarize this paper, we have shown that craters of Lutetia can tell us more about the surface of an asteroid than its age only. Their morphological properties can help us to understand better the local physical properties of the surface. On Lutetia the overall statistics of  $d/D$  is not different from that of any other Solar System object: we found values between 0.05 and 0.3, most of the distribution being in a peak centered around 0.12. We could measure significant variation across the surface, and we interpreted them as differences in structure or evolution of the different regions.

Baetica region appears to have been covered by a deep ejecta blanket which filled most of the preexisting craters. Using the estimated average  $d/D = 0.12$  derived from the global statistics, we calculated the depth of those buried craters for which we could measure the diameter. This leads to a profile of the ejecta thickness around the North pole crater cluster. We integrated this profile to estimate the total amount of material excavated and found that it fits perfectly with a cratering event of the same scale as the one observed in this region. Finally, observations of avalanches in several crater flanks and the presence of many asymmetrical craters with flow-like features, put in perspective with the calculation of local gravity and slopes, are interpreted as evidence for the presence of widespread fine material all over the surface.

## Acknowledgments

OSIRIS was built by a consortium of the Max-Planck-Institut für Sonnensystemforschung, Katlenburg-Lindau, Germany, CISAS

– University of Padova, Italy, the Laboratoire d'Astrophysique de Marseille, France, the Instituto de Astrofísica de Andalucía, CSIC, Granada, Spain, the Research and Scientific Support Department of the European Space Agency, Noordwijk, The Netherlands, the Instituto Nacional de Técnica Aeroespacial, Madrid, Spain, the Universidad Politécnica de Madrid, Spain, the Department of Physics and Astronomy of Uppsala University, Sweden, and the Institut für Datentechnik und Kommunikationsnetze der Technischen Universität Braunschweig, Germany.

The support of the national funding agencies of Germany (DLR), France (CNES), Italy (ASI), Spain (MEC), Sweden (SNSB), and the ESA Technical Directorate is gratefully acknowledged.

We thank the Rosetta Science Operations Centre and the Rosetta Mission Operations Centre for the successful flyby of (21) Lutetia.

We thank the referee for pointing us towards the best scaling laws to describe impact craters on Lutetia, which lead to significant improvement of the paper.

This research has made use of NASA's Astrophysics Data System.

## References

- Asphaug, E., Moore, M., Morison, D., Benz, W., Nolan, M.C., Sullivan, R.J., 1996. Mechanical and geological effects of impact cratering on Ida. *Icarus* 120, 158–184.
- Besse, S., Lamy, P., Jorda, L., Marchi, S., Barbieri, C. Identification and physical properties of craters on asteroid (2867) Steins, submitted for publication.
- Carr, M.H., Kirk, R.L., McEwen, A., Veverka, J., Thomas, P., Head, J.W., Murchie, S., 1994. The geology of Gaspra. *Icarus* 107, 61.
- Chapman, C.R., Ryan, E.V., Merline, W.J., Neukum, G., Wagner, R., Thomas, P.C., Veverka, J., Sullivan, R.J., 1996. Cratering on Ida. *Icarus* 120, 77–86.
- Grieve, 2007. Encyclopedia of the Solar System.
- Hirata, N., Barnouin-Jha, O.S., Honda, C., Nakamura, R., Miyamoto, H., Sasaki, S., Demura, H., Nakamura, A.M., Michikami, T., Gaskell, R.W., Saito, J., 2009. A survey of possible impact structures on 25143 Itokawa. *Icarus* 200, 486–502.
- Housen, K.R., Schmidt, R.M., Holsapple, K.A., 1983. Crater ejecta scaling laws: fundamental forms based on dimensional analysis. *Journal of Geophysical Research* 88 (B3), 2485–2499.

- Housen, K.R., Holsapple, K.A., 2011. Ejecta from impact craters. *Icarus* 211, 856–875.
- Jorda, et al., 2010. Shape and physical properties of asteroid 21 Lutetia from OSIRIS images. In: AAS DPS Meeting #42.
- Keller, H.U., et al., 2007. OSIRIS the scientific camera system onboard Rosetta. *Space Science Reviews* 128, 433–506.
- Keller, H.U., et al., 2010. E-type asteroid (2867) Steins 470 as imaged by OSIRIS onboard Rosetta. *Science* 327, 190.
- Marchi, S., Barbieri, C., Küppers, M., Marzari, F., Davidsson, B., Keller, H.U., Besse, S., Lamy, P., Mottola, S., Massironi, M., Cremonese, G., 2010. The cratering history of asteroid (2867) Steins. *Planetary and Space Science* 58 (9), 1116–1123.
- Marchi, S., Massironi, M., Vincent, J.-B., Morbidelli, A., Barbieri, C., Besse, S., Küppers, M., Marzari, F., Mottola, S., Naletto, G., Sierks, H., Thomas, N. The cratering history of asteroid (21) Lutetia. *Planetary and Space Science*, doi:10.1016/j.pss.2011.10.010, this issue.
- Massironi, M., Thomas, N., Marchi, S., Tubiana, C., Snodgrass, C., Vincent, J.-B., Pajola, M., Da Deppo, V., The OSIRIS Team. Geological map and stratigraphy of asteroid 21 Lutetia. *Planetary and Space Science*, doi:10.1016/j.pss.2011.12.024, this issue.
- Preusker, F., Scholten, F., Knollenberg, J., Kürt, E., Matz, K.-D., Mottola, S., Roatsch, T., Thomas, N. The Northern hemisphere of asteroid 21 Lutetia—topography and orthoimages from Rosetta OSIRIS NAC image data. *Planetary and Space Science*, doi:10.1016/j.pss.2012.01.008, this issue.
- Richardson, J.E., Melosh, H.J., Greenberg, R.J., O'Brien, D.P., 2005. The global effects of impact-induced seismic activity on fractured asteroid surface morphology. *Icarus* 179, 325–349.
- Rummel, et al., 1987. Fracture mechanics approach to hydraulic fracturing stress measurements. In: Atkinson (Ed.), *Fracture Mechanics of Rock*, vol. 6, pp. 217–239.
- Shingareva, T.V., Basilevsky, A.T., Shashkina, V.P., Neukum, G., Werner, S., Jaumann, R., Giese, B., Gwinner, K., 2008. In: *Lunar and Planetary Institute Science Conference Abstracts*, vol. 39, p. 2425.
- Sierks, et al. Images of asteroid 21 Lutetia: a remnant planetesimal from the early solar system. *Science*, accepted for publication.
- Sullivan, R., et al., 1996. Geology of 243 Ida. *Icarus* 120, 119–139.
- Thomas, P., et al., 2002. Eros: shape, topography, and slope processes. *Icarus* 155, 18–37.
- Thomas, N., Barbieri, C., Keller, H.U., Lamy, P., Rickman, H., Rodrigo, R., Sierks, H., Wenzel, K.P., Cremonese, G., Jorda, L., Marzari, F., Massironi, M., Preusker, F., Scholten, F., Stephan, K., Barucci, A., Besse, S., Fornasier, S., Groussin, O., Hviid, S.F., Koschny, D., Kürt, E., Küppers, M., Marchi, S., Martelto, E., Moissl, R., Snodgrass, C., Tubiana, C., Vincent, J.-B. The geomorphology of 21 Lutetia: results from the OSIRIS imaging system onboard ESA's Rosetta spacecraft. *Planetary and Space Science*, doi:10.1016/j.pss.2011.10.003, this issue.
- Veverka, et al., 1999. Imaging of asteroid 433 Eros during NEAR's flyby reconnaissance. *Science* 285 (5427), 562–564.
- Veverka, et al., 2000. NEAR encounter with asteroid 253 Mathilde: overview. *Icarus* 140, 3–16.